Coupled weak ferromagnetic-paramagnetic excitations in $(Gd_{0.5}Eu_{0.5})_2CuO_4$

1992 J. Phys.: Condens. Matter 4 1581

(http://iopscience.iop.org/0953-8984/4/6/024)

J. Phys.: Condens. Matter 4 (1992) 1581–1593. Printed in the UK

Coupled weak ferromagnetic–paramagnetic excitations in $(Gd_{0.5}Eu_{0.5})_2CuO_4$

A Fainstein†, M Tovar†‡ and Z Fisk§

† Centro Atómico Bariloche and Instituto Balseiro, 8400 San Carlos de Bariloche, Rio Negro, Argentina

‡ Instituto de Ciencia de Materiales, CSIC, Campus UAB, 08193 Bellaterra, Spain

§ Los Alamos National Laboratory, Los Alamos, New Mexico 87545, USA

Received 3 June 1991, in final form 9 September 1991

Abstract. The electron paramagnetic resonance spectra of Gd^{3+} in single crystals of $(Gd_{0.5}Eu_{0.5})_2CuO_4$ show an anomalous anisotropy for temperatures below the magnetic ordering of the Cu ions ($T \simeq 280$ K). We have performed a detailed experimental study of this feature, and we discuss our results in terms of a model that assumes a weak Heisenberg interaction between Cu and Gd moments. We show that that anisotropy is a consequence of the dynamic coupling of the Gd^{3+} paramagnetic mode with a weak ferromagnetic mode originating in the Cu magnetic moments.

1. Introduction

The rare-earth cuprates, R_2CuO_4, are parent compounds of the electron-doped high T_c superconductors, $R_{2-x}(Ce, Th)_xCuO_4$ [1]. These cuprates form in a tetragonal (T') crystal structure with CuO_2 planes in which oxygen atoms are square planar coordinated about the Cu atoms [2].

Three different types of magnetic interactions have to be considered in the rare-earth cuprates, namely the Cu–Cu, Cu–R and R–R interactions; since their relative magnitude differ considerably, their effects can be separated by measurements in different temperature ranges [3]. For temperatures above 50 K the magnetic properties are mainly due to the Cu–Cu interaction, leading to magnetic ordering of the Cu lattice around 280 K. Below 50 K the effects of the R–Cu and R–R interactions become increasingly important and must be taken into account in order to describe the magnetic behaviour of the system, including the spin reorientation transition around 15 K and the magnetic ordering of the R lattice for some of the rare-earths at lower temperatures [3, 4].

In this work we have restricted our analysis to the high-temperature behaviour, that is, for temperatures above 50 K. In this range, the rare-earth lattice is paramagnetic, and the R–Cu interaction can be considered as a perturbation.

Muon spin rotation and neutron diffraction experiments indicate that antiferromagnetic (AF) order develops below room temperatures for R = Pr, Nd and Sm [5, 6]. The magnetic behaviour is complex for the heavier rare-earths (Eu through Yb) and weak ferromagnetism (WF) has been observed in these compounds [3, 7].

0953-8984/92/061581 + 13 $04.50

The WF component in $(Gd_{0.5}Eu_{0.5})_2CuO_4$ has been interpreted as being due to a combination of both a canting of the Cu moments away from perfect antiferromagnetism, and a polarization of the paramagnetic rare-earth ions, which are coupled to the CuO_2 planes through an effective internal field of about 1 kGauss [3, 4]. The Dzyaloshinski–Moriya (DM) antisymmetric exchange interaction was suggested to be responsible for the canting of the Cu moments [4, 8].

This WF also introduces specific features in the microwave magneto-absorption spectra. In addition to the Gd^{3+} electron–spin resonance (EPR) lines, intense signals have been measured at low fields [3]. These low-field spectral lines were successfully described as ferromagnetic modes associated with the WF component of the Cu lattice, with a model that included the DM interaction [9]. On the other hand, a very unusual anisotropy of the Gd^{3+} EPR signal that appears below the ordering temperature of the Cu magnetic moments, first reported in [3], remains to be understood.

In order to understand the observed behaviour, we have performed a detailed experimental study of the Gd resonance in single crystals of $(Gd_{0.5}Eu_{0.5})_2CuO_4$. In section 2 we present these data. In section 3 we discuss these results in relation to previous data on the DC magnetization and the weak ferromagnetic resonance; we show that a static coupling between the Cu and Gd systems is not enough to understand the observed anisotropy of the Gd^{3+} EPR. In section 4 we introduce a model for this magnetic system. The model is based on the independent excitations of the Cu weak ferromagnetic and the Gd paramagnetic lattices, and a coupling between the Cu and Gd moments is included through a weak scalar exchange interaction. We show that coupled weak ferromagnetic–paramagnetic resonance modes can be derived from it and we give a quantitative account of the data in terms of these mixed excitations.

2. Experimental results

Single crystals of $(Gd_{0.5}Eu_{0.5})_2CuO_4$ were grown from PbO and CuO fluxes as described in [10]. The crystals were thin platelets of typical size $3 \times 3 \times 0.1$ mm^3 with the c-axis (perpendicular to the CuO_2 planes) parallel to the thinnest dimension.

The EPR experiments were performed in a 9.5 GHz spectrometer operating in the conventional derivative absorption mode. The experimental set-up was precisely mounted so that the external field (H_0) could rotate from a plane direction ([110]) to the c-axis. The crystals were mounted in the resonant cavity so that the time dependent microwave excitation field was kept parallel to the CuO_2 planes, and perpendicular to the external magnetic field. These conditions are required for the simultaneous excitation of the two resonance modes, i.e. the WF resonance and the Gd^{3+} EPR [9].

The microwave absorption spectrum of $(Gd_{0.5}Eu_{0.5})_2CuO_4$ at room temperatures, shows one single broad line ($\Delta H_{pp} \cong 2$ kGauss) at $g \cong 2.0$ (resonant field $H_{r,Gd} \cong 3350$ Gauss) that can be assigned to trivalent gadolinium. For temperatures below 280 K, there is an extra strong absorption at $H_{r,WF} \cong 100$ Gauss. In figure 1 we show a typical spectrum, measured at 180 K; the low field absorption associated with a WF mode and the paramagnetic resonance due to the Gd^{3+} ions are observed. DPPH is used as a marker ($g \cong 2.0$). We will only present here data referred to the Gd^{3+} resonance. The properties of the low-field absorption have been extensively discussed in [3] and [9], and we will only give a brief summary of the main features in section 3.

In figure 2 we show the temperature dependence of the resonant field assigned to the EPR of Gd^{3+}, for two directions of the applied external magnetic field H_0, one parallel

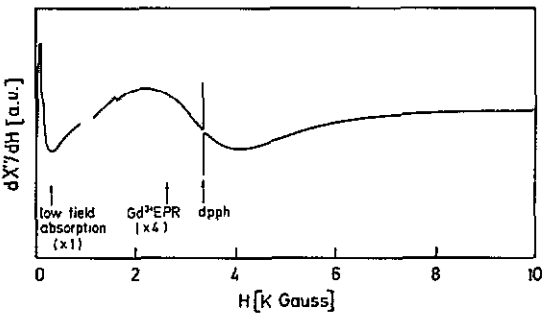

Figure 1. Microwave absorption spectrum for a single crystal of $(Gd_{0.5}Eu_{0.5})_2CuO_4$, measured at 180 K and 9.5 GHz with H_0 applied at 50° from the planes. The low-field absorption associated with a weak ferromagnetic mode and the paramagnetic resonance due to the Gd^{3+} ions are observed. The DPPH is used as a marker.

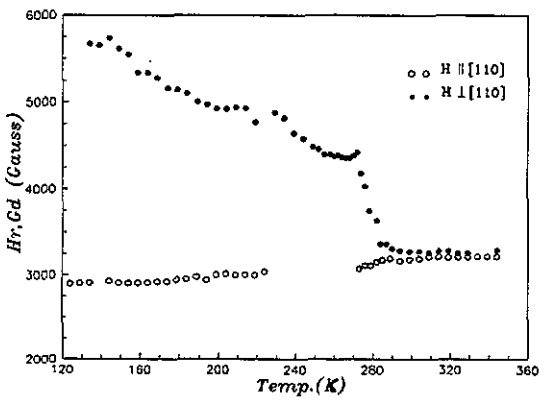

Figure 2. Temperature dependence of the resonant field $H_{r,Gd}$ of the EPR of the Gd^{3+} ion in $(Gd_{0.5}Eu_{0.5})_2CuO_4$ for $\theta = 0°$ and $\theta = 89°$.

to the CuO_2 planes ([110]), and one nearly perpendicular to them (1° from the *c*-axis). $H_{r,Gd}$ was observed to be isotropic in the CuO_2 planes. There is a shift for H_0 applied parallel to the CuO_2 planes, that starts at $T \cong 280$ K and saturates at a field (450 ± 20) Gauss lower than the $g = 2.0$ value. A quite different behaviour is observed for H_0 perpendicular to the CuO_2 planes, where a rapid change is developed, also at $T \cong 280$ K, shifting the resonant field to extreme high values as the temperature is lowered.

This behaviour can be analysed from the angular dependence of the resonant magnetic field as H_0 rotates from [110] to the *c*-axis at a fixed temperature. In figure 3 we show spectra taken at 184 K for different external magnetic field angles θ ($\theta = 0$ for the [110] direction). Both magnetic resonances are shown, the WF mode and the Gd^{3+} signal; it can be seen how both spectral lines shift to higher magnetic fields as the direction of H_0 approaches the *c*-axis, merging together in a single broad absorption for θ close to 90°.

In figure 4 we show the shift of the resonant magnetic field $H_{r,Gd}$ compared with H_{DPPH} (the resonant field corresponding to the DPPH marker) as a function of the angle θ for two temperatures, namely 344 K and 184 K. As shown in figure 2, $H_{r,Gd}$ is nearly independent of angle for $T > 280$ K, whereas for $T < 280$ K an extreme out-of-plane anisotropy is observed. As previously mentioned, $H_{r,Gd}$ is shifted 450 Gauss lower than

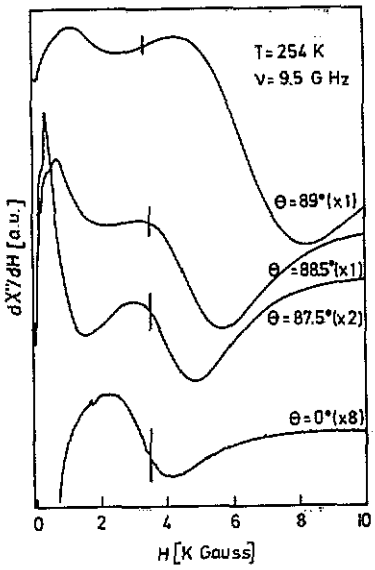

Figure 3. Spectra taken at $T = 184$ K for different external magnetic field angles θ. The two resonances are seen, the Gd^{3+} EPR and the WF resonance. Notice the change of scale.

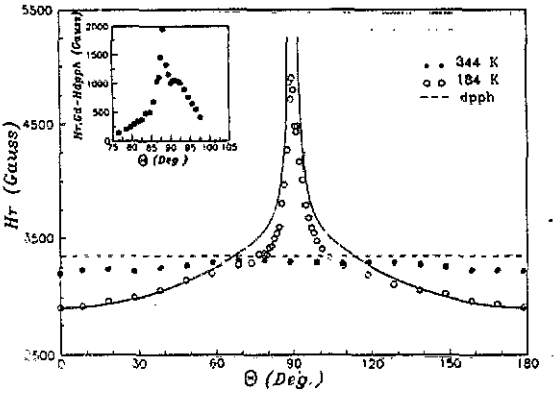

Figure 4. The resonant field $H_{r,Gd}$ of the EPR of the Gd^{3+} ion compared to the $g = 2$ value of the DPPH marker, versus θ, and for $T = 344$ K and $T = 184$ K. The inset shows in detail the region near the c-axis. The full lines correspond to the theoretical model discussed in section 4.

H_{DPPH} for $\theta = 0$, it reaches the value of H_{DPPH} for $\theta \cong 75°$ and continues increasing as θ approaches 90°. Within a few degrees from the c-axis ($\pm 2°$) this behaviour changes and the resonant field drops, defining an asymmetric peaked structure (see inset in figure 4).

As seen in figure 3, another signature of the Gd^{3+} EPR is the strong variation of the intensity of the spectral line with the magnetic field angle θ. In figure 5 we show the angle dependence of the integrated intensity, measured at 184 K. An increase is observed as θ approaches 90°, except for a very narrow range around the c-axis where the intensity drops in a similar way as observed for the resonant magnetic field (see the inset in figure 5). Again, an asymmetric peaked structure is defined around the c-axis.

In figure 6 we show the temperature dependence of the spectral line intensity, for $\theta = 0°$ and $\theta = 89°$. Whereas for H_0 parallel to the CuO_2 planes there are no important changes in the intensity as the temperature is lowered, for H_0 near the c-axis there is an abrupt increase starting at $T \cong 280$ K. This shows that for temperatures above 280 K the intensity is isotropic, while angular dependence, as shown in figure 5, appears as the temperature passes through 280 K.

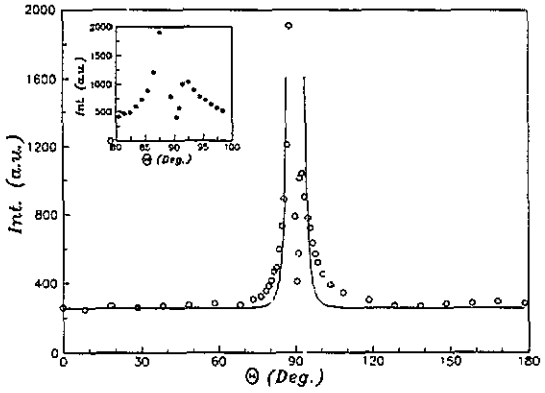

Figure 5. Angular dependence of the intensity of the Gd^{3+} EPR signal at 184 K. The inset shows in detail the drop for $\theta \cong 90°$. The full curves correspond to the theory presented in section 4.

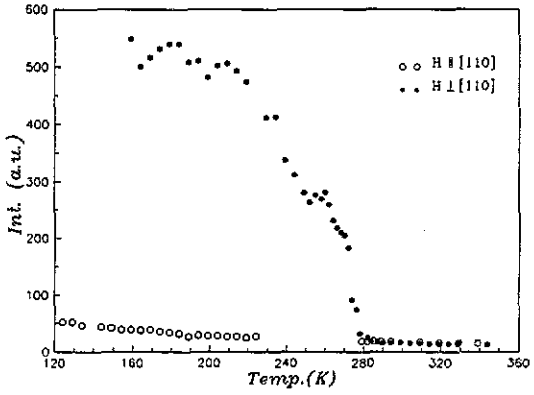

Figure 6. Temperature dependence of the integrated intensity of the EPR of Gd^{3+} for $\theta = 0°$ and $\theta = 89°$.

3. Analysis of the data

In order to discuss the features of the Gd^{3+} magnetic resonance, we will first briefly review previous data on the magnetic properties of $(Gd_{1-x}Eu_x)_2CuO_4$ solid solutions, namely the DC magnetization and the weak ferromagnetic resonance.

3.1. DC magnetization

The DC magnetization (M_{DC}) of these compounds is almost isotropic at room temperatures, and it can be described by the sum of a Curie–Weiss term, for trivalent gadolinium $Gd^{3+}(4f^7; {}^8S_{7/2})$ with $g_{Gd} = 1.991$, and a Van Vleck contribution of the trivalent europium $Eu^{3+}(4f^6; {}^7F_0)$ ions [3, 11].

Below $T \cong 280$ K weak ferromagnetism appears: M_{DC} presents a non-linear behaviour as a function of the applied magnetic field, H_0. Its component parallel to the CuO_2 planes, $M_{\parallel}$, shows an initially fast increase as a function of field and, above a relative small field, H_s, it becomes linear in H_0. H_s defines a minimum external field necessary to develop fully the WF component of the magnetization. Above H_s, $M_{\parallel}$ can be described by the following expression [3, 4],

$$M_{\parallel}(T) = M_{Cu}(T) + [C_{Gd}/(T + T_N)][H_0 + H_{i,Gd}(T)] + M_{Eu}(T) \qquad (1)$$

where $M_{Cu}(T)$ is a WF component of the Cu magnetic moments, originated in a small

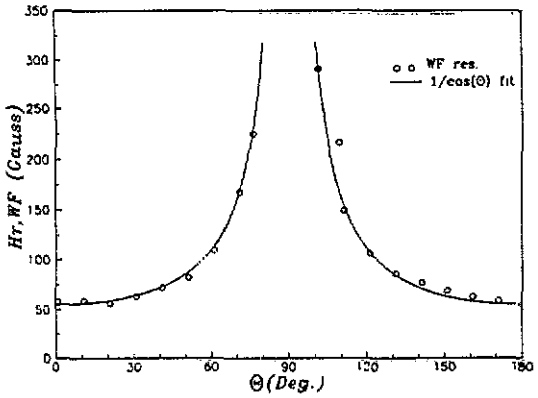

Figure 7. The resonant magnetic field $H_{r,WF}$ of the WF mode as a function of the magnetic field angle θ, at 260 K. The full curve is a fit to the form $H_r(\theta) = H_r(0)/\cos(\theta)$.

departure of strictly AF alignment, $H_{i,Gd}$ is an internal effective field that polarizes the Gd paramagnetic lattice and is due to the Cu WF component, and $M_{Eu}(T)$ is the Eu^{3+} Van Vleck contribution to the magnetization. For $(Gd_{0.5}Eu_{0.5})_2CuO_4$, the estimated values of M_{Cu} and $H_{i,Gd}$ are $M_{Cu} = 2(2) \times 10^{-3}\mu_B$/Cu-atom and $H_{i,Gd} \cong 800$ Gauss [3].

We assume that the presence of Eu has no determinant effect on the observed behaviour of the Gd^{3+} EPR. In fact, similar experiments in Gd_2CuO_4 show exactly the same features. We have chosen $(Gd_{0.5}Eu_{0.5})_2CuO_4$ for the presentation of the characteristics of the Gd^{3+} EPR spectra because the spectral lines are narrower than in Gd_2CuO_4 and so the features we want to stress are more clear in order to compare them with the model in section 4.

The angular dependence of M_{DC} in single crystal measurements suggests that the internal field $H_{i,Gd}$ is constant and orientated within the CuO_2 planes. Besides, from the angular dependence of H_s, it can be deduced that only the component parallel to the CuO_2 planes of the applied magnetic field is effective in the process of developing the measured weak ferromagnetic component.

3.2. Weak ferromagnetic resonant mode

The main features of this resonant mode are [3, 9] as follows.

(i) It appears at about the same temperature where the WF component of the DC magnetization appears ($T \cong 280$ K).

(ii) A strong out-of-plane anisotropy dominates the angular dependence of the resonant field, $H_{r,WF}(\theta)$ (see figure 7), and the peak-to-peak linewidth, $\Delta H_{pp}(\theta)$. Both follow the functional law $f(\theta) = f(0)/\cos(\theta)$, where θ is the angle between H_0 and the CuO_2 planes.

This resonance was described in [9] as a weak ferromagnetic mode, associated with the Cu system and characterized by the following resonance equation, first derived by Pincus [12]

$$(\omega_{WF}/\gamma)^2 = H_0 \cos(\theta)(H_0 \cos(\theta) + H_{DM}) \tag{2}$$

where γ is the gyromagnetic factor appropriate for the Cu moments, and H_{DM} is the so-called Dzyaloshinski–Moriya field, that phenomenologically describes the effect of the antisymmetric DM interaction. The $\cos(\theta)$ factor in (2) arises from a strong anisotropy

energy term favouring the orientation of the Cu moments within the CuO_2 planes, and is the origin of the $1/\cos(\theta)$ dependence in $H_{r,WF}$.

In order to obtain coincident values of H_{DM} from DC magnetization and the analysis of the WF mode, it is necessary to introduce the coupling to the Gd lattice through an effective field 'seen' by the Cu moments. H_{DM} was estimated to be of the order of 10^5 Gauss [9].

Based on the above results we will now discuss the characteristics of the Gd^{3+} EPR; we will analyse separately three features of the data, i.e. the resonant field $H_{r,Gd}$, the integrated intensity of the spectral line, and the near *c*-axis region defined in the angular variations.

3.3. The resonant magnetic field

Above 280 K, the resonant field is nearly isotropic and corresponds to $g \cong 2$, in agreement with the magnetization data. Below 280 K, specific features appear associated with the weak ferromagnetism. DC magnetization measurements show that an internal field $H_{i,Gd}$, due to the Cu system, is acting along the CuO_2 planes at each Gd site. This internal field is expected to produce a shift of the resonant field. The observed shift of $H_{r,Gd}$ at $\theta = 0$ (450 Gauss) is in the right direction but is significantly smaller than the 800 Gauss obtained from DC magnetization measurements. On the other hand, it can be expected that the value $H_r - H_{DPPH}$ would go to zero at $\theta \cong 90°$; instead, a divergent behaviour is observed as the direction of H_0 approaches the *c*-axis.

This divergence can be represented by a $1/\cos(\theta)$ behaviour near the *c*-axis, this feature being a signature of the WF mode. It should be noted that the hypothesis that leads to the angular dependence of $H_{r,WF}$ in (2), namely the anisotropy that favours the orientation of the Cu magnetic moments parallel to the CuO_2 planes, cannot be used here since the Gd^{3+} ions are in a paramagnetic state and follow the magnetic field.

It is clear that the anisotropy of the Gd^{3+} resonance has to be related to the magnetic ordering of the Cu moments, but a static coupling, represented by the internal field $H_{i,Gd}$ obtained from the DC magnetization, does not explain the observed features.

3.4. The intensity

The integrated intensity of an electron paramagnetic resonance depends on three factors, namely the number of resonating magnetic moments, their magnitude, and the transition probability.

Angular dependence of the transition probabilities can appear in systems with a high crystalline anisotropy, but this can be ruled out in our case since, above the temperature of the magnetic ordering of the Cu moments, the integrated intensity is isotropic.

The number of Gd^{3+} ions is constant and their magnitude depends on temperature with a Curie–Weiss law; hence it would be expected that there is a $1/T$ dependence of the intensity, as in fact is observed when H_0 is applied parallel to the CuO_2 planes, but not the strong anisotropy that appears below 280 K, shown in figures 5 and 6.

An internal field would only shift the resonance, but would not produce an angular dependence of the intensity; hence, another mechanism associated with a coupling between the Gd and Cu magnetic lattices must be considered.

3.5. The central region

In the angular dependence of $H_{r,Gd}$ (see figure 4) and the angular dependence of the integrated intensity (see figure 5) below 280 K, a centre region is defined around the c-axis ($\theta \cong 90° \pm 2°$) where both $H_{r,Gd}$ and the intensity change their overall behaviour. Two features related to this centre region must be analysed, namely the drop for $\theta \cong 90°$, and the asymmetry of the formed peaked structure.

Although not evident, the mechanism that gives rise to the observed anisotropy must be related to the appearance of weak ferromagnetism at 280 K. Hence, the drop observed when the direction of H_0 is nearly parallel to the c-axis, can be interpreted as a consequence of there no longer being a large enough component of the field applied in the plane to 'set' fully the weak ferromagnetism.

We do not have a complete explanation for the origin of the asymmetry, but at least two mechanisms have to be considered: (i) the non-perfect alignment between the external magnetic field H_0 and the c-axis, as θ passes through 90°; and (ii) the angular modulation of the absorption. Angular modulation arises when H_0 and the modulation field used for lock-in signal detection are not aligned. It can be important in very anisotropic resonances [13] and since it depends on the angular derivative of the resonant field, $\partial H_r(\theta)/\partial\theta$, its contribution to the total intensity of the signal must change sign as the c-axis is crossed by H_0. In order to evaluate the importance of this experimental feature, we have repeated the same measurements changing the angle φ between H_0 and the modulation field. We observed that, although the general characteristics of the angular dependence of $H_{r,Gd}$ and the intensity do not change, the detail of the central part, i.e. the relative magnitude of the peaks, is sensitive to changes as small as 1° in φ.

4. Theoretical model

The anomalous behaviour described above can be explained in terms of a coupled mode of the Gd and Cu magnetic lattices. Mode mixing results in new excitations analogous to polaritons or magneto-elastic modes [14, 15].

Figure 8 shows the expected angular dependence of the individual Gd and Cu excitations and the mixed modes derived from them. The resonant fields for the individual modes, and hence their resonant frequencies in a given field, are well separated when θ is close to 0° or 180° but become degenerate at some angle close to 90°. We may therefore expect the modes to preserve their independent character when the field lies in or near to a [110] direction, whereas strong coupling will occur when the field direction is close to the c-axis.

In what follows, we will show that this resonant coupling of modes can be derived on the basis of weakly interacting Gd and Cu magnetic lattices, coupled through an isotropic Heisenberg Hamiltonian.

We will consider not the individual magnetic moments but the macroscopic magnetization fields, of the Gd paramagnetic lattice (M_{Gd}), and of the Cu WF lattice (M_{Cu}). The macroscopic field theory is specially appropriate for magnetic resonance [14], where, since the excitation field $H_1(t) = H_1 e^{i\omega t}$ is uniform in space, only $k = 0$ magnons can be excited.

We propose a zero-order energy that describes the system,

$$\mathcal{H}_0 = E_0 + \omega_{WF} c^+ c + \omega_{PM} g^+ g \tag{3}$$

where E_0 is the equilibrium energy, $c^+|0\rangle$ is a state of one $k = 0$ WF magnon with energy

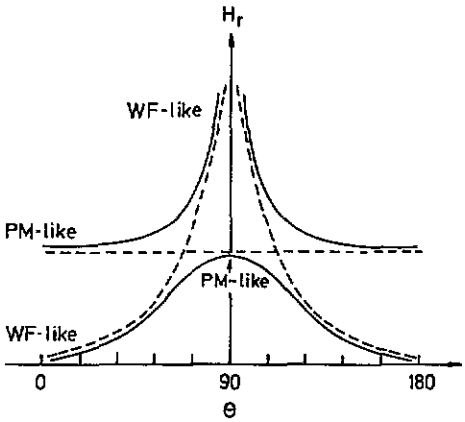

Figure 8. Schematic diagram of the coupled modes of a WF $k = 0$ magnon and a paramagnetic excitation. The broken lines show the behaviour without interaction. Notice that the lower branch of the mixed excitations is WF-like when $\theta \cong 0°$ or 180° but becomes PM-like when $\theta \cong 90°$, while the upper branch is PM-like when H_0 is near to a [110] direction but WF in character when the c-axis is approached (see section 4).

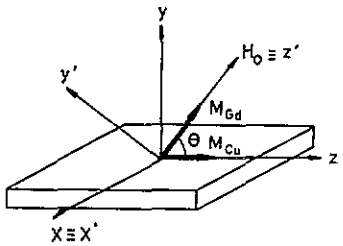

Figure 9. Ground states used in the model. The WF magnetization M_{Cu} is taken parallel to the planes and in the direction of the plane component of the external field H_0; the paramagnetic magnetization M_{Gd} follows the field H_0 as it rotates an angle θ from the CuO_2 planes.

given by (2) and $g^+|0\rangle$ is a state of one paramagnetic excitation with energy $\omega_{PM} = \gamma H_0$ (we take $\hbar = 1$).

For the coupling between the Gd and Cu magnetic moments we assume

$$\mathcal{H}_{int} = -\lambda \boldsymbol{M}_{Gd} \cdot \boldsymbol{M}_{Cu}. \tag{4}$$

We define the mean internal fields $\boldsymbol{H}_{i,Gd} = \lambda \boldsymbol{M}_{Cu}$ as due to the copper moments acting on the Gd sites, and $\boldsymbol{H}_{i,Cu} = \lambda \boldsymbol{M}_{Gd}$ of the Gd magnetic moments acting on the Cu magnetic moments. $\boldsymbol{H}_{i,Gd}$ and $\boldsymbol{M}_{Gd}$ can be obtained from DC magnetization measurements. The constant λ can be related to the exchange constant J_{Cu-Gd} on a molecular field basis. If we assume that Gd ions interact mainly with the four near neighbour copper ions, and since $M_{Cu} \cong 2 \times 10^{-3} \mu_B$/Cu-atom and $H_{i,Gd} \cong 800$ Gauss [3], we can estimate $J_{Cu-Gd}/k_B \cong 30$ K.

Equation (4) can be written in terms of creation and annihilation operators using the Holstein–Primakoff transformation [14]. In that case, each magnetization must be referred to a different frame of axes: we assume that disregarding small perturbations $\boldsymbol{M}_{Cu}$ is parallel to the CuO_2 planes, while $\boldsymbol{M}_{Gd}$ follows the external field as it moves away from the planes to a direction perpendicular to them (see figure 9). The total energy $\mathcal{H} = \mathcal{H}_0 + \mathcal{H}_{int}$ can then be written as the sum of the following terms,

$$\begin{aligned}
\mathcal{H}_{dd} &= [\omega_{WF} + \gamma\lambda M_{Gd}\cos(\theta)]c^+c + [\omega_{PM} + \gamma\lambda M_{Cu}\cos(\theta)]g^+g \\
\mathcal{H}_{\uparrow\downarrow} &= -(\gamma\lambda/2)(M_{Cu}M_{Gd})^{1/2}(1 + \cos(\theta))[cg^+ + c^+g] \\
\mathcal{H}_{\uparrow\uparrow} &= -(\gamma\lambda/2)(M_{Cu}M_{Gd})^{1/2}(1 - \cos(\theta)) \quad [cg + c^+g^+] \\
\mathcal{H}_{ZY} &= -(\lambda/2i)\sin(\theta)[M_{Gd}(2\gamma M_{Cu})^{1/2}(c - c^+) - M_{Cu}(2\gamma M_{Gd})^{1/2}(g - g^+)]
\end{aligned} \tag{5}$$

where M_{Cu} and M_{Gd} are the modulus of the magnetizations. Constant contributions to the total energy are not included.

Although, in principle, it is possible to obtain the eigenvalues of the entire energy $\mathcal{H}$, more insight on the physical meaning of the solution can be obtained by separately analysing each term in (5).

The diagonal part $\mathcal{H}_{dd}$ includes the energies of the independent modes shifted by the internal fields, as expected from a mean field static approach.

The second term $\mathcal{H}_{\downarrow\uparrow}$ with non-diagonal terms cg^+ and c^+g, corresponds to the annihilation of one type of excitation with the simultaneous creation of an excitation of the other system. These terms are typical of resonantly coupled modes; $\mathcal{H}_{dd} + \mathcal{H}_{\downarrow\uparrow}$ can be diagonalized with the transformation $\alpha^+ = ug^+ + vc^+$ and $\beta^+ = vg^+ - uc^+$ with u and v real numbers, and where $\alpha^+|0\rangle$ and $\beta^+|0\rangle$ correspond to mixed states. The energies of these mixed excitations are

$$\omega\pm = (\omega^*_{WF} + \omega^*_{PM})/2 \pm \{[(\omega^*_{WF} - \omega^*_{PM})/2]^2 + \omega_I^2\}^{1/2} \tag{6}$$

where the ω^* are the independent frequencies shifted by the internal fields, and $\omega_I = (\lambda\gamma/2)(M_{Cu}M_{Gd})^{1/2}(1 + \cos(\theta))$ is the interaction term that couples both modes. The value of ω_I is always non-zero since θ varies only from 0° to 90°. Even for small values of ω_I it cannot be considered just as a perturbation since, as can be seen from (6), ω_I has to be compared with the difference of both diagonal frequencies, $\Delta\omega^*$. In fact, when $\omega^*_{WF} = \omega^*_{PM}$ a gap opens with an energy difference of $2\omega_I$. In this way, two separate branches are obtained as shown in the schematic diagram in figure 8.

This resonant coupling can also be seen analysing the eigenvectors; the constants u and v that diagonalize $\mathcal{H}_{dd} + \mathcal{H}_{\downarrow\uparrow}$ are

$$\begin{aligned} u^2 &= 1/2 \pm [(1/2)^2 - A]^{1/2} \\ v^2 &= 1/2 \mp [(1/2)^2 - A]^{1/2} \end{aligned} \tag{7}$$

where

$$A = \omega_I^2/[(\omega^*_{WF} - \omega^*_{PM})^2 + 4\omega_I^2].$$

If the frequency difference $\Delta\omega^*$ is much larger than ω_I then $A \cong 0$ and there are two solutions for each α or β: $u = 0$ and $v = 1$ or $u = 1$ and $v = 0$, i.e. the eigenstates correspond essentially to the independent excitations. If $\Delta\omega^* = 0$ then $u^2 = v^2 = 1/2$ and the eigenstates α and β correspond to a mixing of the paramagnetic and weak ferromagnetic modes, both with the same weight. The lower branch in figure 8 is weak ferromagnetic-like when θ is close to 0° or 180°, and becomes paramagnetic-like for $\theta \cong 90°$, while the upper branch, that we associate with the Gd^{3+} EPR, is paramagnetic-like when the field is near to a [110] direction, but becomes weak ferromagnetic in character when the field direction is close to the c-axis.

The third term of (4), $\mathcal{H}_{\uparrow\uparrow}$, with non-diagonal operators cg and c^+g^+ corresponds to the simultaneous creation or annihilation of both types of excitations. It is zero for $\theta = 0$, corresponding to the ferromagnetic alignment of both magnetic systems, but similarly to the case of antiferromagnetic magnons [14] they show that for a non-ferromagnetic situation the Néel state is not the exact ground state and point-zero oscillations appear. It can be diagonalized with $\mathcal{H}_{dd}$ using the Bogoliubov transformation $\alpha = uc - vg^+$ and $\beta = ug - vc^+$. The diagonal energies in this case are

$$\omega \pm = \pm(\omega^*_{WF} - \omega^*_{PM})/2 + \{[(\omega^*_{WF} + \omega^*_{PM})/2]^2 + \omega_{II}^2\}^{1/2} \tag{8}$$

with $\omega_{II} = (\lambda\gamma/2)(M_{Cu}M_{Gd})^{1/2}(1 - \cos(\theta))$. The case now is different from the preceding

one; ω_{II} is zero for H_0 in the plane and it can be considered as a perturbation since it has to be compared with the sum of the independent excitation energies. In fact, when $\omega_{II} \ll \omega^*_{WF} + \omega^*_{PM}$ (8) can be expanded to give

$$\omega_{+(-)} \cong \omega^*_{WF(PM)} - \omega^2_{II}/(\omega^*_{WF} + \omega^*_{PM}). \tag{9}$$

Equation 9 shows that the two energies are lowered by the same amount, and that the shift can be considered as a perturbation. The eigenvectors can be analysed calculating the numbers u and v; it can be shown that the new states α and β differ from the independent excitations c and g also in order $\omega_{II}/(\omega^*_{WF} + \omega^*_{PM})$.

The last term of (5) generates only a shift in the constant part of the total energy H and does not need to be considered in order to describe the excitations of the system.

Since we have shown that $H_{\uparrow\uparrow}$ can be taken as a perturbation, and that the reduced energy $H \cong H_{dd} + H_{\uparrow\downarrow}$ contains the necessary elements to describe the coupling of modes, in what follows we will only consider these two terms for a more quantitative approach.

We first consider the case for H_0 parallel to the CuO_2 planes, i.e. $\theta = 0°$. If, in (6), we assume that $\Delta\omega^* \gg \omega_I$, the frequency of the paramagnetic mode corrected by the interaction can be shown to be

$$\omega/\gamma \cong H_0 + H_{i,Gd} - H_{i,Cu}H_{i,Gd}/([H_0(H_0 + H_D)]^{1/2} + H_{i,Cu} - H_0 - H_{i,Gd}). \tag{10}$$

Equation (10) shows that the resonant field will be shifted not only by $H_{i,Gd}$ as expected from a static approach, but that there is also a shift that makes $H_{r,Gd}$ go to higher values and is originated in the dynamic coupling of the two modes. If we assume that this is the origin of the difference between the measured shift of $H_{r,Gd}$ for $\theta = 0$ (450 Gauss) and $H_{i,Gd}$ (800 Gauss), we can obtain from this model a value for H_{DM} since all other terms in (6) or (10) are already known. From our data at $T = 184$ K we get $H_{DM} \cong 10^5$ Gauss, which is in agreement with the value estimated from DC magnetization and the weak ferromagnetic resonance.

With this value for H_{DM}, the resonant field of the signal assigned to the Gd^{3+} EPR can be calculated for any external field angle θ, from (6), with no free parameters. In figure 4 we show the experimental results for the angular dependence of this resonance at $T =$ 184 K, with the theoretical curve deduced from this model (full curves); the agreement is remarkable, reproducing the observed divergent behaviour.

A quantitative estimation of the angular dependence of the integrated intensity of the spectral line can also be obtained from our model. Since the eigenstate we are exciting is defined by $\alpha^+|0\rangle = ug^+|0\rangle + vc^+|0\rangle$, with u and v given in (7), the intensity of the absorption due to the coupled mode can be obtained as

$$I_\alpha(\theta) = u^2 I_{Gd}(\theta) + v^2 I_{Cu}(\theta) \tag{11}$$

where $I_{Gd}(\theta)$ and $I_{Cu}(\theta)$ are the intensities of the absorptions expected for the independent modes.

Following the discussion in section 3, we assume that $I_{Gd}(\theta) = I_{Gd}(0)$, with $I_{Gd}(0)$ the value of the intensity assigned to the Gd^{3+} EPR at $\theta = 0°$, where $\alpha^+|0\rangle \cong g^+|0\rangle$.

On the other hand, we do not have a model to describe $I_{Cu}(\theta)$. Nevertheless, a phenomenological argument can be given, based on the observed angle dependence of the WF resonance [9]. In fact, when this resonance is clearly separated from the Gd^{3+} EPR line, its peak to peak linewidth varies with θ as $\Delta H_{pp}(\theta) = \Delta H_{pp}(0)/\cos(\theta)$, while its amplitude, h, is nearly constant. The integrated intensity is proportional to $h\Delta H^2_{pp}$;

hence we assume $I_{Cu}(\theta) \cong I_{Cu}(0)/\cos^2(\theta)$, with $I_{Cu}(0)$ the intensity of the WF mode for $\theta = 0°$ where it can be considered as independent.

In figure 5 we show the experimental results for the angular dependence of the intensity of the spectral line assigned to Gd^{3+} at 184 K, with the theoretical curve calculated this way (full curves). Although this model is admittedly oversimplified, the overall behaviour is correctly reproduced. It is clear that a more detailed description of $I_{Cu}(\theta)$ is needed for a precise determination of the expected intensity for the coupled modes. Moreover, the angular variation of the measured intensity due to angular modulation of the absorption, as mentioned in section 3, was not taken into account. Experimental errors in the determination of $I_a(\theta)$ which originated in the superposition of the two observed modes must also be considered.

5. Conclusions

We have presented a detailed experimental investigation of the anomalous behaviour observed on the magnetic resonance assigned to Gd^{3+} in $(Gd_{0.5}Eu_{0.5})_2CuO_4$.

We introduced a model for this magnetic system, that describes these anomalies in terms of a new type of magnetic excitation, i.e. coupled paramagnetic–weak ferromagnetic modes. All of the presented unusual features can be explained considering the following.

(i) The difference between the resonant field with H_0 parallel to the CuO_2 planes and the expected value including the static internal field $H_{i,Gd}$ is interpreted as being due to a dynamic coupling of the modes. From this analysis we obtained $H_{DM} \cong 10^5$ Gauss, which is in agreement with previous results. In fact, it could have been taken as an input to the model.

(ii) The $1/\cos(\theta)$ behaviour of the resonant field $H_{r,Gd}$ is a signature of the weak ferromagnetic character of the upper branch of the mixed excitations when θ approaches 90°.

(iii) The anomalous angular dependence of the intensity of the absorption is a consequence of this mixing. Since the excitations are linear combinations of the independent modes, not only the individual transition probabilities must be considered but also the weight with which each mode enters the mixed state.

(iv) The decrease of $H_{r,Gd}$ and of the intensity, for $\theta \cong 90°$, can also be understood with this model: since for H_0 parallel to the c-axis there is no weak ferromagnetic magnetization, the independent Gd^{3+} excitation must be recovered.

A final test for the model would be the observation of the complete lower branch of figure 8, that is, the WF mode saturating at a resonant field near the $g \cong 2$ value. This is not possible in $(Gd_{0.5}Eu_{0.5})_2CuO_4$, nor in Gd_2CuO_4: broadening of the spectral line and superposition with the Gd^{3+} EPR prevents a precise determination of the resonant field for angles nearer than 10° from the c-axis, and hence critical effects due to the dynamic coupling of modes are not evident.

Acknowledgments

We wish to thank Dr C Fainstein for a critical reading of the manuscript and Dr S B Oseroff and L B Steren for helpful conversations and collaboration. We would also like

to thank the first referee for his thorough reading and useful indications on the first version of this work. We acknowledge partial funding of the research at the Centrol Atómico Bariloche by the Consejo Nacional de Investigaciones Científicas of Argentina and at the Los Alamos National Laboratory by the United States Department of Energy.

References

[1] Tokura Y, Takagi H and Uchida S 1989 *Nature* **337** 345
Takagi H, Uchida S and Tokura Y 1989 *Phys. Rev. Lett.* **62** 1197
Market J T and Maple M B 1989 *Solid State Commun.* **70** 145
Market J T, Early E A, Bjornholm T, Ghamathy S, Lee B W, Neumeier J J, Price R D, Seaman C L and Maple M B 1989 *Physica* C **158** 178

[2] Muller-Buschbaum Hk and Wollschlager W 1975 Z. *Anorg. Allg. Chem.* **414** 76
Grande B, Muller-Buschbaum Hk and Suhweizer M 1977 *ibid* **428** 120

[3] Oseroff S B, Rao D, Wright F, Vier D C, Schultz S, Thompson J D, Fisk Z, Cheong S-W, Hundley M F and Tovar M 1990 *Phys. Rev.* B **41** 1934

[4] Thompson J D, Cheong S-W, Brown S E, Fisk Z, Oseroff S B, Tovar M, Vier D C and Schultz S 1989 *Phys. Rev.* B **39** 6660

[5] Luke G M, Sternlieb B J, Uemura Y J, Brewer J H, Kadona R, Kiefl R F, Kritzman S R, Riseman T M, Gopalakrishnan J, Sleight A W, Subramanian M A, Uchida S, Takagiana H and Tokura Y 1989 *Nature* **338** 49

[6] Allenspach P, Cheong S-W, Dommann A, Fisher P, Fisk Z, Furrer A, Ott H R and Rupp B 1989 Z. *Phys. B.: Condens. Matter* **77** 185
Yoshizawa H, Mitsuda S, Mori H, Yamada Y, Kobayashi T, Sawa H and Akimitsu J 1990 *J. Phys. Japan* **59** 428

[7] Tovar M, Obradors X, Pérez F, Oseroff S B, Duro R J, Rivas J, Chateigner D, Bordet P and Chenavas J 1991 unpublished

[8] Dzyaloshinsky I 1958 *J. Phys. Chem. Solids* **4** 241
Moriya T 1960 *Phys. Rev.* **120** 91
Moriya T 1966 *Magnetism* vol I, ed G T Rado and H Suhl (New York: Academic Press) p 85

[9] Fainstein A, Tovar M and Fisk Z unpublished

[10] Kubat-Martin K A, Fisk Z and Ryan R 1988 *Acta Crystallogr.* **44C** 1518

[11] Tovar M, Rao D, Barnett J, Oseroff S B, Thompson J D, Cheong S-W, Fisk Z, Vier D C and Schultz S 1989 *Phys. Rev.* B **39** 2661

[12] Pincus P 1960 *Phys. Rev. Lett.* **5** 13

[13] Edgar E 1975 *J. Phys. E: Sci. Instrum.* **8** 179

[14] Kittel C 1963 *Quantum Theory of Solids* (New York: Wiley) Ch 3, 4

[15] Wrege D E, Spooner S and Gersch H A 1971 *AIP Conf. Proc. on Magnetism and Magnetic Materials (Chicago, USA, 1971)* **5** 1334